Article

An Amphiphilic, Graphitic Buckypaper Capturing Enzyme Biomolecules from Water

Shahin Homaeigohar * [ID] **and Mady Elbahri ***

Nanochemistry and Nanoengineering, School of Chemical Engineering, Department of Chemistry and Materials Science, Aalto University, Kemistintie 1, 00076 Aalto, Finland
* Correspondence: shahin.homaeigohar@aalto.fi (S.H.); mady.elbahri@aalto.fi (M.E.); Tel.: +358-50-431-9831

check for updates

Abstract: The development of carbon nanomaterials for adsorption based removal of organic pollutants from water is a progressive research subject. In this regard, carbon nanomaterials with bifunctionality towards polar and non-polar or even amphiphilic undesired materials are indeed attractive for further study and implementation. Here, we created carbon buckypaper adsorbents comprising amphiphilic (oxygenated amorphous carbon (a-CO_x)/graphite (G)) nanofilaments that can dynamically adsorb organic biomolecules (i.e., urease enzyme) and thus purify the wastewaters of relevant industries. Given the dynamic conditions of the test, the adsorbent was highly efficient in adsorption of the enzyme (88%) while being permeable to water (4750 $L \cdot h^{-1} m^{-2} bar^{-1}$); thus, it holds great promise for further development and upscaling. A subsequent citric acid functionalization declined selectivity of the membrane to urease, implying that the biomolecules adsorb mostly via graphitic domains rather than oxidized, polar amorphous carbon ones.

1. Introduction

As a global challenge, water scarcity is expanding to major parts of the world, threatening human beings' lives. This crisis can have different origins but undoubtedly water pollution from industry and from urban communities is a main one. Amongst the variety of water pollutants, the organic ones such as proteins and biomolecules play a determining role. These substances even at a negligible amount, <1% of the entire contamination in a river, for instance, can deplete the oxygen present in water and cause the death of living creatures in that ecosystem [1]. Water recycling via purification can somewhat remediate this problem but necessitates the development of advanced water treatment systems. Micro-, ultra- and nanofiltration membranes are typically utilized for wastewater treatment. Their purification action mainly relies on sieving of the pollutants, and thus they require a porous structure whose pore size is less than the size of the solute to be separated. Other than the membranes, in a sustainable manner and using conventional and also emerging materials, functionalized adsorbents have shown applicability in the removal of even molecules and tiny pollutants based on physical/chemical interactions or biological functions [2–7]. Accordingly, there is no need for the construction of porous materials with small pore sizes that could impose high pressure differences. Moreover, a functionalized adsorbent with a surface decorated by particular functional groups can discriminate or entrap molecules in a selective manner [8].

Electrospun nanofibrous adsorbents have shown promising capabilities for selective water remediation. Their structure possesses a high interconnected porosity and huge surface area that in case of functionalization can efficiently separate functional pollutants, e.g., ions, dye molecules, organics, etc. While the high porosity realizes a significant permeability and with that, energy efficiency, the expansive surface area enables the notable functionalization necessary for highly selective

adsorbents. In this regard, several biofunctionalized nanofibrous membranes made of polyurethane, polysulfone, polyacrylonitrile, and cellulose have been tested for the separation of protein and enzyme (e.g., Immunoglobulin G (IgG), Bovine Serum Albumin (BSA), lipase, bromelain, etc.) [8–11]. In our studies [2,4,12], we also developed a biofunctionalized nanofibrous adsorbent composed of Bovine Serum Albumin and poly(acrylonitrile-co-glycidyl methacrylate) (PANGMA), as the functional agent and polymer nanofiber, respectively, that could offer a significant metal nanoparticle and biomolecule removal efficiency while being highly water permeable. This adsorbent was synthesized in a simple fashion versus the other previously developed systems [8,13]. The separation tests were performed under the most tricky conditions, i.e., dynamically and with a low protein amount (a few mg·L^{-1} instead of mg·mL^{-1} adopted by References [8,10,11,14]) and with a size scale of pollutants, potentially passing readily through a macroporous nanofibrous structure. Despite such circumstances, the adsorbent was successful in the removal of nanoparticles (97%) as well as proteins (88% BSA and 81% *Candida antarctica* Lipase B (Cal-B)). In another research, we developed a nanofibrous adsorbent comprising polyethersulfone (PES) nanofibers that were functionalized by the inclusion of vanadium oxide (V_2O_5) nanoparticles [6]. This adsorbent system was able to separate methylene blue (MB) dye from water with an efficiency of 85% under alkaline condition and high temperature.

Despite the various merits of the above-mentioned systems in the adsorption of diverse water pollutants, their synthesis and functionalization are not one pot. As a step forward to meet this need, recently, we developed carbon buckypapers based on amphiphilic carbon nanofilaments [15]. The nanofilaments are composed of oxygenated amorphous carbon (a-CO_x) and graphite (G), and thus are able to adsorb both polar (e.g., dye) and non-polar (e.g., oil) water pollutants efficiently. Already investigating the applicability of the amphiphilic graphitic buckypaper in discrimination of polar and non-polar contaminants, here, we challenge the buckypaper adsorbents with an amphiphilic water pollutant. For this sake, biomolecules (i.e., urease enzyme), one of the major organic pollutants that can adversely affect the water ecosystems, will be considered.

2. Experimental

Materials: polyacrylonitrile (PAN) (200,000 g·mol^{-1}, purity 99.5%) and dimethylformamide (DMF) (purity 99%) were purchased from Dolan GmbH (Kelheim, Germany) and Merck (Darmstadt, Germany), respectively. Urease enzyme (impurity; ammonium < 4–10 µmol·U^{-1} enzyme) and citric acid (citric acid monohydrate, ACS reagent ≥ 99.0%) were obtained from Sigma-Aldrich (Saint Louis, MO, USA). All the materials were used as received.

Synthesis: The precursor PAN nanofibers were synthesized by electrospinning. To do so, employing a syringe pump (Harvard Apparatus, Holliston, MA, USA), a solution of PAN (8 wt % in DMF) was fed steadily (1 mL·h^{-1}) into a needle (0.8 mm inner diameter with a circular opening). Upon electrifying the solution with a voltage of 20 kV (Heinzinger Electronic GmbH, Rosenheim, Germany), PAN was electrospun on an aluminum foil. The as-synthesized PAN nanofibers underwent oxidative stabilization and were heated in air at 250 °C for 2 h within a furnace with maximum operational temperature of 1250 °C (Linn Elektro Therm). In the next step, the oxidized nanofibers were carbonized under argon atmosphere at 1250 °C for half an hour with a heating rate of 5 °C·min^{-1} and then cooled down to the room temperature at a same rate.

Due to the extreme brittleness of the graphitized nanofibers, challenging their handling as a freestanding membrane, they were suspended in distilled water (10 mL) and underwent an ultrasonication process for 2 min at a power of 20%. The a-CO_x/G nanofibers under the influence of ultrasonication are disintegrated as suspended nanofilaments that can be subsequently cast on a circular poly(phenylene sulfide) (PPS) technical nonwoven (3.5 cm in diameter). As a control group, a-CO_x/G nanofilaments were also functionalized by citric acid (CA). To do this, CA (30 mg·mL^{-1})) was added to the aqueous suspension to be ultrasonicated.

Characterization: The a-CO_x/G nanofilaments were characterized in terms of morphology by scanning electron microscopy (SEM) (LEO 1550VP Gemini from Carl ZEISS, Jena, Germany) and an

atomic force microscope (AFM) (MultiMode$^{\text{TM}}$ Atomic Force Microscope from Bruker AXS, Madison, WI, USA). The surface chemistry of the a-CO$_x$/G nanofilaments was analyzed by FTIR (ALPHA (ATR-Ge, ATR-Di) from BRUKER Optik GmbH, Ettlingen, Germany). The a-CO$_x$/G buckypaper's pore size distribution was determined by an automated capillary flow porometer (Porous Materials Inc. (PMI), Ithaca, NY, USA).

The urease retention efficiency of the buckypapers was assessed using the corresponding aqueous solutions in a dead-end manner and by employing a lab-built set-up [16]. The set-up's reservoir contained 200 mL urease solution (1 g·L^{-1}) which permeated through the buckypapers under a 0.5 bar pressure. Based on a constructed standard urease calibration curve, the permeate's urease concentration was determined by UV-vis spectroscopy (HITACHI U3000, HITACHI, Tokyo, Japan). The urease retention efficiency (RE) was calculated via Equation (1):

$$RE = \left(1 - \frac{C_p}{C_f} \right) \times 100\% \tag{1}$$

where C_p and C_f represent the permeate's and feed's urease concentration, respectively. The permeation time was also recorded and the permeate permeance was calculated via Equation (2) [17]:

$$J = \frac{Q}{A \times \Delta t \times \Delta P} \tag{2}$$

where J is the permeate permeance (L·h^{-1}m^{-2}bar^{-1}), Q is the collected volume (L) of the permeate, A is the effective filtration area of the buckypapers (m^2), Δt is the collecting time (h), and ΔP is the pressure difference (bar). The permeance measurements were done for three 50 mL permeates to ascertain the consistency of the buckypapers' performance. It is worthy to note that considering the hydrophobic, large microfibers of the PPS support layer, providing huge pore sizes, no significant contact and interaction with the urease molecules passing through the carbon layer can be envisioned. Thus, only the buckypaper is responsible for the reported removal efficiency and permeance.

The electrical conductivity of the buckypapers as non-functionalized and CA-functionalized before and after urease adsorption was measured by a four-point probe test. At least five measurements were done on different parts of the buckypapers, and the error bars were calculated. The thickness of the samples to be considered in the conductivity measurement was already measured by a digital micrometer (Deltascope®MP2C from Fischer, Windsor, CT, USA).

3. Results and Discussion

The developed buckypaper consists of the a-CO$_x$/G nanofilaments, randomly arranged but with no sign of clustering. SEM image, as shown in Figure 1a, clearly verifies this fact and the preservation of a porous structure that guarantees optimum water permeability. Moreover, as seen in Figure 1b, the nanofilaments' tips are exposed to the surrounding medium, and thus, this raises the interactivity of the material with the biomolecule pollutants. In fact, the nanofilaments are able to capture urease through adsorption not only on their body, but also on their cross-sections. AFM images, as shown in Figure 1c, provide insight into the dimensions and morphology of the nanofilaments individually.
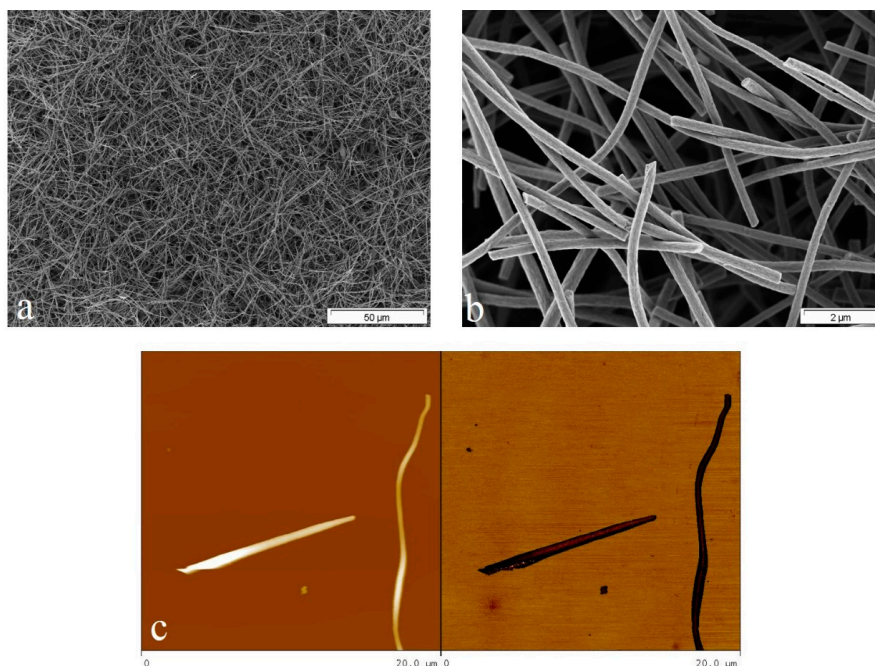
Figure 1. Scanning electron microscopy (SEM) images show morphology of the nanofilaments at (**a**) a low and (**b**) high magnification. (**c**) Atomic force microscope (AFM) micrographs imply the nanofilaments' dimensions and morphology.

Pore size measurement via a bubble point test, as shown in Figure 2, implies that the pore size lies in the submicron range as small as 700 nm. This pore size distribution qualifies the structure as a microfiltration (MF) membrane [18,19] that could hardly stop the passage of tiny organic pollutants, particularly under hydrodynamic pressure. It is worthy to note that the adsorption tests reported in the literature are typically performed in a static, batch mode that maximizes the contact time of the adsorbent and solutes. To the contrary, here, we adopted an adsorption test in a dynamic mode under a hydrodynamic pressure that could challenge the adsorption efficiency of our samples. This test was performed in three successive steps, in each, 50 mL of the solution was passed through. Such a style can highlight the repeatability of the result and also stress robust bonding of the urease molecules with the nanofilaments in case they are not released in the next steps and if efficiency does not decline.
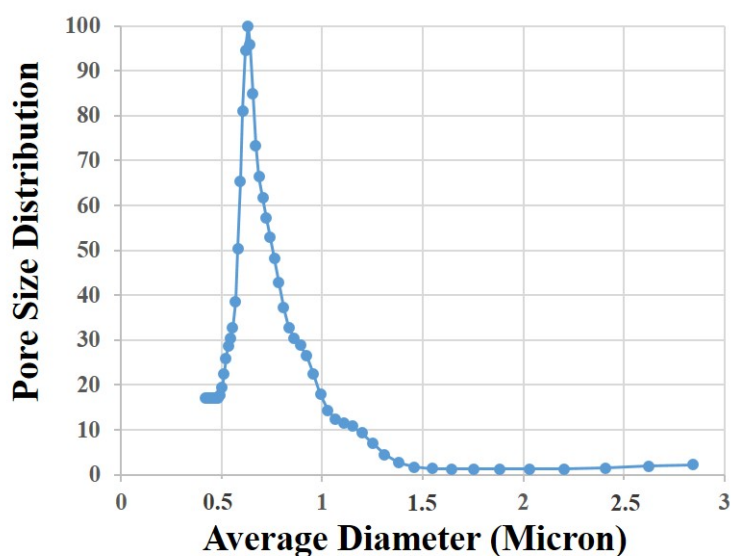

Figure 2. Pore size distribution of the a-CO$_x$/G buckypaper measured by a bubble point test.

Despite possessing pore sizes in the MF scale, the buckypaper showed a promising urease separation efficiency, as shown in Figure 3a. A removal efficiency of 88.5% was recorded after permeation of 150 mL urease aqueous solution. An ascending trend from 50 mL (75%) to 150 mL (88%) in urease removal efficiency is observed. As we previously proved [15], the nanofilaments have oxygen-based functional groups including carbonyl and hydroxyl that enable interaction, i.e., hydrogen bonding with amino acid units of urease. In addition to hydrogen bonding, the positively charged amine groups of urease and the negatively charged oxygen-based functional groups of a-CO_x segments can electrostatically interact. On the other hand, major graphitic regions allow for π-π interaction with non-polar domains of urease. For a similar DNA–CNT system, van der waals forces have been introduced as an adsorption driving factor with a larger impact than hydrophobic forces [20]. For the urease molecules, several intramolecular bondings between different functional groups could also be envisaged. Accordingly, some molecules interact through their less polar and non-polar zones with the nanofilaments. Thus, collectively, different parts of the nanofilaments are able to adsorb urease molecules via interaction with their corresponding regions. This feature can stabilize the enzyme on its substrate and prevent its conformational change that can lead to loss of enzyme activity, which is beneficial for further application as, e.g., a biocatalyst [21–23]. Moreover, the huge surface area of the buckypaper minimizes the diffusion pathway for the reaction products, thus enhancing the efficiency of the immobilized enzyme. ATR-FTIR spectra, as shown in Figure 4a, clearly verify the adsorption of urease onto the nanofilaments. Before the adsorption, the strong peak located at 1589 cm^{-1} represents the unoxidized sp^2 C=C groups of the graphitic segments of the nanofilaments, which resulted from the aromatization process during the thermostabilization of PAN nanofibers [24,25]. The second evident groups at 1000–1300 (two bands) and 3800 cm^{-1} imply a C–OH bond [15]. After the adsorption, the main chemical bonds related to urease emerge on the nanofilaments. These bonds represented by ATR-FTIR characteristic peaks are marked in Figure 4a.
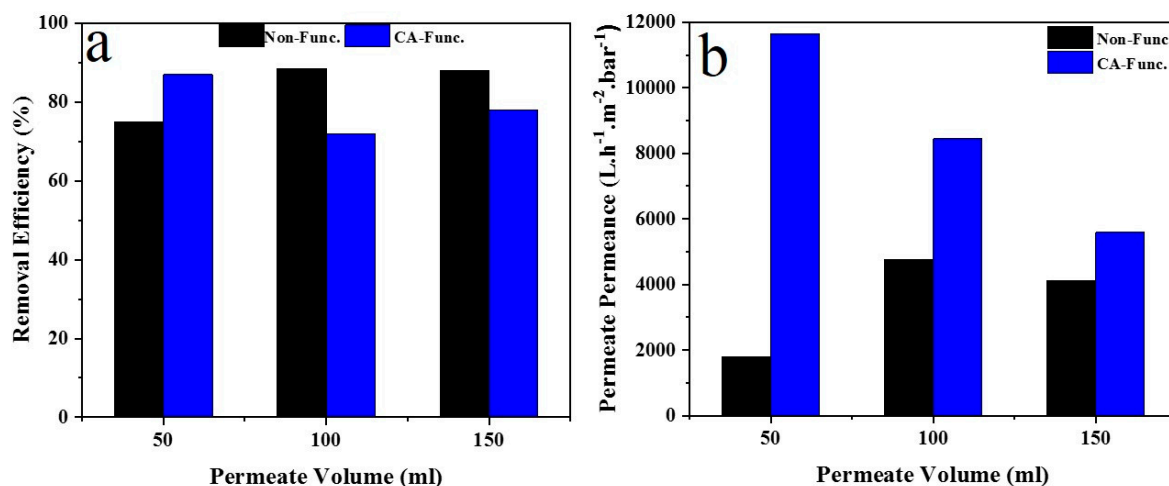

Figure 3. (**a**) Urease removal efficiency; (**b**) permeate permeance of the buckypapers in two classes of non-functionalized and CA-functionalized.
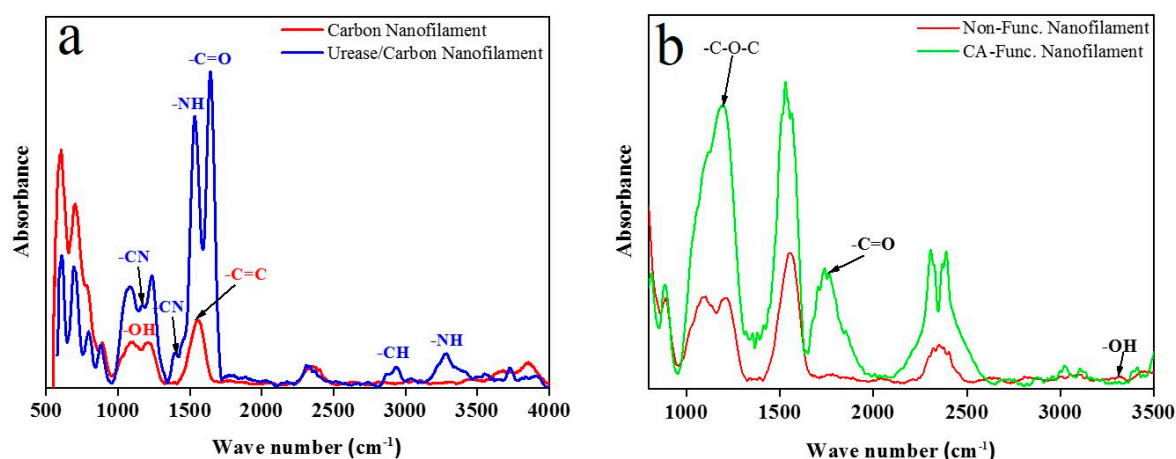
Figure 4. ATR-FTIR spectra compare the surface chemistry of carbon nanofilaments before and after (**a**) urease adsorption and (**b**) CA functionalization.

The increasing trend of urease removal efficiency shows that the adsorption of urease is robust and further passage of the solution does not result in its release into water. This enhancement of removal efficiency can be attributed to a strong intermolecular interaction between the adsorbed urease molecules and solutes via peptide–peptide interactions [26]. Interestingly, adsorption of urease molecules enhances permeate permeance of the buckypaper after the first round, due to a hydrophilization effect, as shown in Figure 3b. It is worthy to note that the pure water permeance of non- and CA-functionalized were measured as $\approx$8670 and 14000 (L·h^{-1}m^{-2}bar^{-1}), respectively, and adsorption of urease declines, most likely due to pore blockage and loss of porosity. In contrast to the non-functionalized samples, CA-functionalization and the emergence of various functional groups such as carboxyl and hydroxyl (Figure 4b) slightly lower the removal efficiency as far as the filtration is continued. While a high efficiency of 87% is seen at the onset of the experiment, it declines to 78% at 150 mL permeate volume. The reason could be found at less available binding sites for urease molecules or even the release of the previously adsorbed ones because of less graphitic regions that most likely have played a more important role in the stable adsorption of urease molecules rather than polar groups (hydrogen bonding or electrostatic interaction). However, still efficiency is as promising as 78%. It is worth nothing that permeate permeance for CA-buckypapers are significantly higher than that for the non-functionalized ones due to their hydrophilicity. The descending trend of permeate permeance in this class of adsorbents could be attributed to their declined hydrophilicity compared to the neat or fresh CA-functionalized samples due to the adsorption of the urease molecules. Slightly enhanced hydrophobicity along with the accumulation of the adsorbed molecules on the nanofilaments that lower pore size, cooperatively increase the resistance against water permeation.

The adsorption experiment performed here can be regarded as a proof of concept witnessing the applicability of the buckypaper adsorbent in the removal of urease molecules as a model for biomolecule pollutants from water. In this regard, taking into account the effect of environmental factors such as pH, temperature, ionic strength, adsorption time, and urease concentration, further experiments are in progress. The results will be later used in isotherm, thermodynamic and kinetic calculations. There is also a need for more strict tests considering a diverse range of pollutants, different applied stresses and environmental conditions that can affect the separation performance of such an adsorbent. In this regard, software-assisted design of experiments could be helpful. It can reduce the consumption and waste of chemicals, help with regards to the eco-friendliness of chemical processes and actually shorten the pathway to industrial applications [27,28].

As an extra bonus, the enzyme immobilization successfully performed here can be promising for further applications of the buckypaper with respect to biosensing, e.g., the buckypaper adsorbent can potentially act as a biosensor as well. Adsorption of urease can change the electrical conductivity

of the nanofilaments, and thus, the entire buckypaper. To validate this proof of concept, electrical conductivity of the buckypaper before and after adsorption of urease was recorded. As shown in Figure 5, CA functionalization can lower the electrical conductivity of the buckypaper due to the inclusion of carboxyl groups that act as electron-withdrawing elements, raising electrical resistivity. In contrast, adsorption of urease enhances the electrical conductivity notably, but with a lower rate for CA-functionalized buckypapers. One reason for the enhancement of conductivity could be the formation of electron transfer bridges between the nanofilaments by urease molecules. This observation can be interpreted in another way, i.e., bridging between enzyme molecules (i.e., the biosensing element) by the carbon nanofilaments. This phenomenon, i.e., the direct electrical connection of redox enzymes and electrodes through carbon nanomaterials have been reported earlier. Patolski et al. [29] showed this behavior through the alignment of glucose oxidase enzymes on the SWCNTs' tips that were structured as an array on a conductive substrate. Exposure of the enzyme-immobilized buckypaper to the urea, often monitored in blood to track kidney diseases, can alter the electrical conductivity and be considered as the sensing mechanism for such an analyte. It is worthy to note that the immobilization of enzymes is indeed the simplest technique that can tackle the bottleneck of their high solubility [30]. Enzyme immobilization allows for the tailoring of the bioreactions' conditions, and thus enables a continuous process with minimum pollution by the reaction products, an extremely desirable characteristic in the food industry. Moreover, it guarantees an improved stability, lifespan and ease of removal of the enzyme from the reaction medium at the end of the process, enabling cost effectiveness and recycling of the enzyme. As mentioned earlier, immobilization can also lead to stabilization of biocatalysts, prevent their unfolding and immunize the polypeptide bonds against rupture.
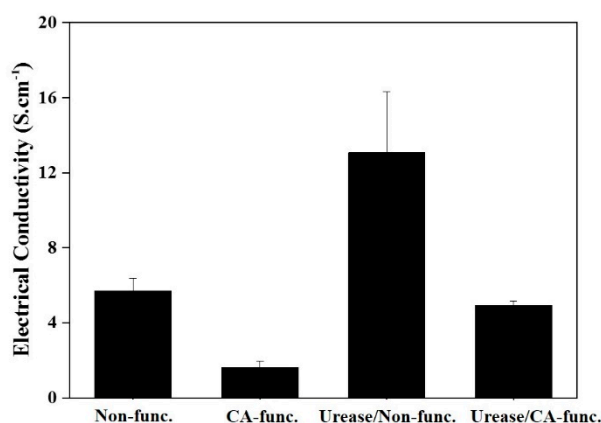

Figure 5. Electrical conductivity of the various classes of buckypapers before and after the adsorption of urease measured via a four-probe test.

4. Conclusion

Taken together, we devised a buckypaper adsorbent based on amphiphilic carbon nanofilaments that could separate urease molecules from water effectively (as large as 88%). The separation tests were performed under dynamic conditions that could challenge the adsorbent more strictly. Desirable selectivity and permeance (over $4 \text{ kL·h}^{-1}\text{m}^{-2}\text{bar}^{-1}$) of this novel adsorbent/membrane holds great promise for further development of the system for practical applications. Furthermore, firm immobilization of urease on conductive nanofilaments can assure the efficiency of a potential biosensing system. This proof of concept makes us optimistic with respect to the high potential of such nanomaterials for water treatment and biosensing in an industrial platform. However, first, we need to tackle some relevant bottlenecks for upscaling of their production. Electrospinning has shown to be a reliable method for large scale production of nanofibers, but post treatment (i.e., carbonization) of nanofibers must be performed in a controlled manner following a precise protocol that can govern a desirable chemistry for nanofibers. This step must be optimized and designed in a more economical way. For instance, the as-developed carbon nanofibers need to be stronger to exclude

the chopping step, while maintaining their uniformity, porosity and more importantly functionality. We are at the beginning of the development of this system for water treatment and biosensing, but the obtained results encourage and motivate us to start further working on our material either as is or coupled with extra reactive agents.

Author Contributions: S.H. conceived the idea, prepared samples, performed characterizations and drafted the manuscript. M.E. was involved in development of the idea and analysis of the results.

Conflicts of Interest: The authors declare no conflict of interest. The founding sponsors had no role in the design of the study; in the collection, analyses, or interpretation of data; in the writing of the manuscript, and in the decision to publish the results.

References

1. Ramakrishna, S.; Fujihara, K.; Teo, W.-E.; Yong, T.; Ma, Z.; Ramaseshan, R. Electrospun nanofibers: Solving global issues. *Mater. Today* **2006**, *9*, 40–50. [CrossRef]
2. Homaeigohar, S.; Dai, T.; Elbahri, M. Biofunctionalized nanofibrous membranes as super separators of protein and enzyme from water. *J. Colloid Interface Sci.* **2013**, *406*, 86–93. [CrossRef]
3. Homaeigohar, S.; Davoudpour, Y.; Habibi, Y.; Elbahri, M. The electrospun ceramic hollow nanofibers. *Nanomaterials* **2017**, *7*, 383. [CrossRef]
4. Homaeigohar, S.; Disci-Zayed, D.; Dai, T.; Elbahri, M. Biofunctionalized nanofibrous membranes mimicking carnivorous plants. *Bioinspir. Biomim. Nanobiomater.* **2013**, *2*, 186–193. [CrossRef]
5. Homaeigohar, S.; Elbahri, M. Nanocomposite electrospun nanofiber membranes for environmental remediation. *Materials* **2014**, *7*, 1017–1045. [CrossRef]
6. Homaeigohar, S.; Zillohu, A.U.; Abdelaziz, R.; Hedayati, M.K.; Elbahri, M. A novel nanohybrid nanofibrous adsorbent for water purification from dye pollutants. *Materials* **2016**, *9*, 848. [CrossRef]
7. Razali, M.; Kim, J.F.; Attfield, M.; Budd, P.M.; Drioli, E.; Lee, Y.M.; Szekely, G. Sustainable wastewater treatment and recycling in membrane manufacturing. *Green Chem.* **2015**, *17*, 5196–5205. [CrossRef]
8. Ma, Z.W.; Kotaki, M.; Ramakrishna, S. Electrospun cellulose nanofiber as affinity membrane. *J. Membr. Sci.* **2005**, *265*, 115–123. [CrossRef]
9. Bamford, C.H.; Allamee, K.G.; Purbrick, M.D.; Wear, T.J. Studies of a novel membrane for affinity separations: I. Functionalization and protein coupling. *J. Chromatogr.* **1992**, *606*, 19–31. [CrossRef]
10. Ma, Z.; Kotaki, M.; Ramakrishna, S. Surface modified nonwoven polysulphone (PSU) fiber mesh by electrospinning: A novel affinity membrane. *J. Membr. Sci.* **2006**, *272*, 179–187. [CrossRef]
11. Zhang, H.; Nie, H.; Yu, D.; Wu, C.; Zhang, Y.; White, C.J.B.; Zhu, L. Surface modification of electrospun polyacrylonitrile nanofiber towards developing an affinity membrane for bromelain adsorption. *Desalination* **2010**, *256*, 141–147. [CrossRef]
12. Elbahri, M.; Homaeigohar, S.; Dai, T.; Abdelaziz, R.; Khalil, R.; Zillohu, A.U. Smart metal-polymer bionanocomposites as omnidirectional plasmonic black absorbers formed by nanofluid filtration. *Adv. Funct. Mater.* **2012**, *22*, 4771–4777. [CrossRef]
13. Ma, Z.; Lan, Z.; Matsuura, T.; Ramakrishna, S. Electrospun polyethersulfone affinity membrane: Membrane preparation and performance evaluation. *J. Chromatogr. B-Anal. Technol. Biomed. Life Sci.* **2009**, *877*, 3686–3694. [CrossRef]
14. Lu, P.; Hsieh, Y.-L. Lipase bound cellulose nanofibrous membrane via Cibacron Blue F3GA affinity ligand. *J. Membr. Sci.* **2009**, *330*, 288–296. [CrossRef]
15. Homaeigohar, S.; Strunskus, T.; Strobel, J.; Kienle, L.; Elbahri, M. A flexible oxygenated carbographite nanofilamentous buckypaper as an amphiphilic membrane. *Adv. Mater. Interfaces* **2018**, *5*, 1800001. [CrossRef]
16. Homaeigohar, S.S.; Mahdavi, H.; Elbahri, M. Extraordinarily water permeable sol gel formed nanocomposite nanofibrous membranes. *J. Colloid Interface Sci.* **2012**, *366*, 51–56. [CrossRef]
17. Lee, H.D.; Kim, H.W.; Cho, Y.H.; Park, H.B. experimental evidence of rapid water transport through carbon nanotubes embedded in polymeric desalination membranes. *Small* **2014**, *10*, 2653–2660. [CrossRef]

18. Baker, R. *Membrane Technology and Applications*, 2nd ed.; Wiley: Chichester, UK, 2004.

19. Homaeigohar, S.S.; Buhr, K.; Ebert, K. Polyethersulfone electrsopun nanofibrous composite membrane for liquid filtration. *J. Membr. Sci.* **2010**, *365*, 68–77. [CrossRef]

20. Gao, H.; Kong, Y.; Cui, D.; Ozkan, C.S. Spontaneous insertion of DNA oligonucleotides into carbon nanotubes. *Nano Lett.* **2003**, *3*, 471–473. [CrossRef]

21. Pogorilyi, R.; Melnyk, I.; Zub, Y.; Seisenbaeva, G.; Kessler, V. Immobilization of urease on magnetic nanoparticles coated by polysiloxane layers bearing thiol-or thiol-and alkyl-functions. *J. Mater. Chem. B* **2014**, *2*, 2694–2702. [CrossRef]

22. Azevedo, A.M.; Prazeres, D.M.; Cabral, J.M.; Fonseca, L.P. Stability of free and immobilised peroxidase in aqueous–organic solvents mixtures. *J. Mol. Catal. B Enzym.* **2001**, *15*, 147–153. [CrossRef]

23. Villeneuve, P.; Muderhwa, J.M.; Graille, J.; Haas, M.J. Customizing lipases for biocatalysis: A survey of chemical, physical and molecular biological approaches. *J. Mol. Catal. B Enzym.* **2000**, *9*, 113–148. [CrossRef]

24. Hu, M.; Mi, B. Enabling graphene oxide nanosheets as water separation membranes. *Environ. Sci. Technol.* **2013**, *47*, 3715–3723. [CrossRef]

25. Singh, G.; Rana, D.; Matsuura, T.; Ramakrishna, S.; Narbaitz, R.M.; Tabe, S. Removal of disinfection byproducts from water by carbonized electrospun nanofibrous membranes. *Sep. Purif. Technol.* **2010**, *74*, 202–212. [CrossRef]

26. Barisci, J.N.; Tahhan, M.; Wallace, G.G.; Badaire, S.; Vaugien, T.; Maugey, M.; Poulin, P. Properties of carbon nanotube fibers spun from DNA-stabilized dispersions. *Adv. Funct. Mater.* **2004**, *14*, 133–138. [CrossRef]

27. Weissman, S.A.; Anderson, N.G. Design of experiments (DoE) and process optimization. A review of recent publications. *Org. Process Res. Dev.* **2015**, *19*, 1605–1633. [CrossRef]

28. Valtcheva, I.B.; Marchetti, P.; Livingston, A.G. Crosslinked polybenzimidazole membranes for organic solvent nanofiltration (OSN): Analysis of crosslinking reaction mechanism and effects of reaction parameters. *J. Membr. Sci.* **2015**, *493*, 568–579. [CrossRef]

29. Patolsky, F.; Weizmann, Y.; Willner, I. Long-range electrical contacting of redox enzymes by SWCNT connectors. *Angew. Chem.* **2004**, *116*, 2165–2169. [CrossRef]

30. Schoemaker, H.E.; Mink, D.; Wubbolts, M.G. Dispelling the myths—Biocatalysis in industrial synthesis. *Science* **2003**, *299*, 1694–1697. [CrossRef]